Photoinduced domain-type collective structural changes with interlayer σ-bonds in the visible region of graphite

Hiromasa Ohnishi[1,*] and Keiichiro Nasu[1,2]

[1]*Solid State Theory Division, Institute of Materials Structure Science, High Energy Accelerator Research Organization (KEK), 1-1, Oho, Tsukuba, 305-0801, Japan*

[2]*Graduate University for Advanced Study and CREST JST, 1-1, Oho, Tsukuba, 305-0801, Japan*

(Received 24 November 2008; revised manuscript received 26 January 2009; published 24 February 2009)

We theoretically study the photoinduced domain-type structural changes in the visible region of graphite. By means of the *ab initio* total-energy calculation, we clarify the adiabatic path for the nucleation of this domain, wherein the interlayer distance of the original graphite is contracted and new interlayer σ-bonds are induced with a certain periodic buckling pattern. We show that an excitation by few visible photons is energetically enough to trigger the formation of this domain, and this domain is sufficiently stable against the thermal fluctuation at around room temperature. The electronic state of this domain is also shown to have a pseudogap, characteristic to an insulator immersed in the original semimetallic graphite.

DOI: 10.1103/PhysRevB.79.054111 PACS number(s): 78.67.−n, 73.20.At, 71.30.+h

I. INTRODUCTION

It is now well known that some materials exhibit their structural changes by the irradiation of a few visible lights. Electrons just after excited by lights are usually in the Franck-Condon state with no lattice motion from the starting ground state. However, they afterward induce a motion of surrounding lattice because of a sudden change in their charge distribution. As a result, the whole system reaches a different phase in the excited states as a cooperative phenomenon including these electrons and the lattice. This type of nonequilibrium phase transition is known as the photoinduced structural phase transition (PSPT), being one of the promising phenomena to reveal varieties of hidden properties in materials that cannot be observed in ordinary equilibrium phases.[1–3]

The graphite is a well-known material and its unique property attracts much interest from solid-state physics to engineerings. A single graphite layer, a graphene, has the honeycomb lattice and its electronic state exhibits semimetallic nature constructed by the sp^2 bond. Each graphene is very weakly bounded by the van der Waals force in the graphite crystal.

The recent experiment by Kanasaki *et al.*[4,5] revealed the appearance of a photoinduced phase in this graphite by the irradiation of visible photons. The scanning tunneling microscopy (STM) measurement shows a nanoscale domain, in which one third of carbons sinks down and residual two thirds rise up from the layer in each six-membered ring. Carbons that have sunk down are expected to form σ-bonds between graphite layers, whereby the sp^3-like structure is induced. Here we briefly recapitulate the essential experimental aspects. (1) The exciting laser, with the energy 1.57 eV, should be polarized perpendicular to the graphite layers, while the one polarized parallel to the graphite layer gives no effect. (2) The exciting light should be a femtosecond pulse, while the picosecond one gives almost no contribution. (3) The process is a quite nonlinear but less than the ten-photon process. (4) The resultant domain includes more than 1000 carbons and is stable for more than 10 days at room temperature. A similar experiment was performed by Raman *et al.*[6] Their electron-diffraction investigation revealed that the interlayer distance after the photoirradiation has contracted up to 1.9 Å from the original 3.35 Å.

One can easily infer that this phenomenon is closely related to the graphite-diamond conversion that has been energetically studied by various theories and experiments.[7–14] The graphite phase is the true ground state of the macroscopically condensed carbon system and the energy difference from the diamond is only 0.02 eV/atom.[7] The energy barriers between them are about 0.3 eV/atom for the rhombohedral (*ABC* stacking) graphite-cubic diamond transformation[8,10] and about 0.4 eV/atom for the hexagonal (*AB* stacking) graphite-hexagonal diamond transformation.[9,10] They are estimated by the total-energy calculation with the local-density approximation (LDA). Above calculations, however, assume that the whole macroscopic carbons uniformly transform from the graphite to the diamond. To trigger such a transition, a macroscopic order of energy is also required, and the corresponding process is realized by the application of a high temperature and a high pressure (3000 °C, 15 GPa) (Refs. 11 and 12) or strong x ray.[13,14]

The present photoinduced phenomenon is entirely different from such a global and macroscopic phase transition. The present structure is realized only through iterative local domain formation by a successive visible photon excitation, wherein only a finite and microscopic order of energy is required. The resultant domain is nanosized and is still surrounded by the semimetallic continuum of the original graphite. In this case, an incommensurate energy at the domain boundary surely exists and its appropriate treatment is a key theoretical issue. The present domain structure—thus appeared—is not the conventional diamond, but an intermediate state between the graphite and the diamond. Hence we will tentatively refer it as "diaphite" hereafter for the convenience of explanation.

As mentioned before, electrons just after excited by lights are usually in the Franck-Condon state with no lattice motion from the starting ground state. However, they afterward in-

duce a motion of surrounding lattice because of a sudden change in their charge distribution. As a result, the whole system reaches a different state in the excited states as a cooperative phenomenon including these electrons and the lattice.

The whole process of this PSPT will be a very complicated one. This process surely starts from the graphite, and the destination may be the diamond. In between, however, there may be various local minima in the adiabatic potential-energy surface spanned by the multidimensional lattice distortion coordinates of carbons.

Then, in this paper, we will be mainly concerned only with the minimal domain; in the sense, it is expected to be the most nearest potential minimum from the starting graphite in this multidimensional potential surface. As mentioned before, we call this domain as "diaphite." Then, we will clarify the adiabatic path to nucleate this minimal diaphite domain, starting from the perfect graphite, by means of the *ab initio* total-energy calculation with the LDA. The electronic state of the estimated diaphite will also be clarified by means of the tight-binding (TB) approximation with the Slater-Koster (SK) parametrization.[15] We will also clarify the stability of the diaphite by comparing it with a few other competitive distortion patterns.

This paper is organized as follows. In Sec. II, the strategy of the total-energy calculation is explained and the estimated adiabatic potential is given. In Sec. III, we clarify the stability of the diaphite by comparing with a few other competitive buckling states. In Sec. IV, the electronic state of the diaphite that is estimated in Sec. II is clarified by using the TB approximation. Its method is also explained. In Sec. V, not the minimal but a more higher-energy state is clarified as a reference state to study the effect of the local shear displacement. Finally, in Sec. VI, we make a conclusion.

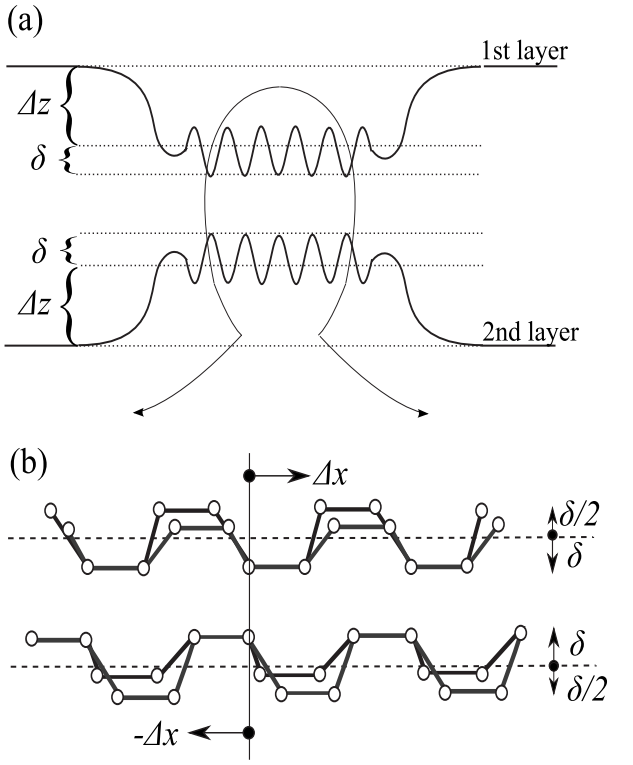

FIG. 1. A schematic picture of the trial distortion pattern. (a) The disk-type intrusion from the graphite layer. (b) The buckling pattern inside the domain inferred from the STM image. One third of carbons sinks down with the amplitude δ and two thirds of carbons rise up with the amplitude $\delta/2$ in each six-membered ring, so as to keep its center of mass unchanged. Then the total intrusion from the graphite layer is given as $(\Delta z+\delta)$. The local shear displacement is introduced to the opposite direction in each layer. Its value at the domain center is referred to Δx.

II. ADIABATIC PATH FOR THE DIAPHITE FORMATION

To estimate the adiabatic path to nucleate the minimal diaphite domain, we have performed the *ab initio* total-energy calculation with the LDA of the form of the Slater exchange[16] and the VWN1 correlation[17] functionals. The used wave function is the linear combination of atomic orbital (LCAO) form based on the Gaussian STO-3 G.[18] Our numerical implementation is basing on the GAMESS code.[19] The exchange-correlation potential is evaluated by partitioning the multicenter integrals into single-center subintegrals[20] with the 63 points of the radial grid in the Euler-MacLaurin quadrature and the 302 points of the angular grid in the Lebedev quadrature. The self-consistent field (SCF) convergence is achieved by the Pulay's direct inversion in the iterative subspace (DIIS) method.[21]

To take into account the local domain formation, we have performed the calculation on a large carbon cluster with a two-layer *AB*-stacking structure which consists of 294 carbons per layer. We have not applied the periodic boundary condition, since the locally deformed lattice breaks the translational symmetry of the system, and each cluster boundary in *ab* plane has been terminated by hydrogens. We start with the complete graphite structure with the intralayer bond distance 1.42 Å and the interlayer bond distance 3.35 Å. The local deformation of the lattice is introduced by taking into account the following displacements. (1) The disk-type intrusion $\Delta z(>0)$ from the graphite surface, perpendicular to the graphite layers. (2) The buckling amplitude $\delta(\geq 0)$; two thirds of carbons rise up and one third of carbons sinks down in each six-membered ring, keeping its center of mass unchanged. (3) The local shear displacement $\Delta x(>0)$; each layer is shifted to the opposite direction to improve the interlayer stacking sequence. A schematic picture of this deformation pattern is given in Fig. 1. Here we define the domain as the region that the carbons sunk down more than $\Delta z/2$, and the number of carbons in this domain is referred to as N_d. The structure of the domain boundary is optimized at each domain size.

The estimated adiabatic energy surface for the nucleation of the diaphite domain in the graphite is given in Fig. 2. The energy is always referenced from that of the starting complete graphite throughout this paper, and the $(\Delta z+\delta)$ is the total intrusion from the graphite surface as shown in Fig. 1(a). The red line represents the minimal ascending path from the starting graphite to the present structure. It is just guide for the eyes. The real formation process is the Franck-Condon excitation, and the lattice relaxation therefrom; it

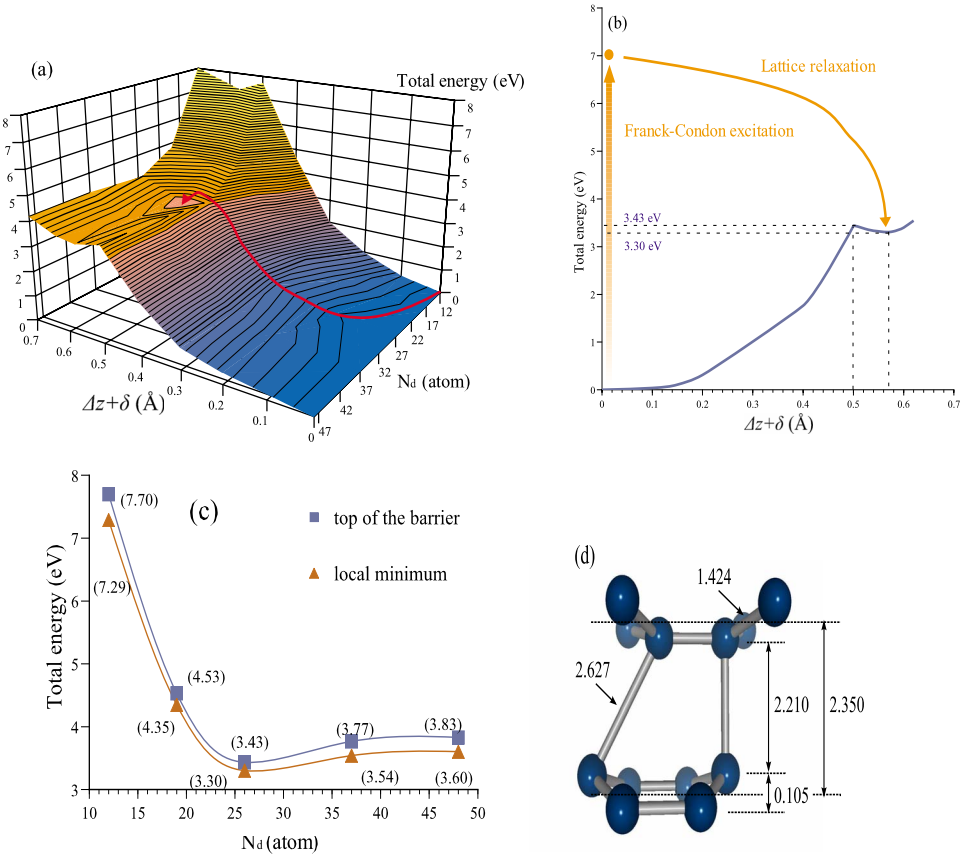

FIG. 2. (Color online) The adiabatic path to the diaphite. The energy is referenced from that of the starting complete graphite. (a) The adiabatic energy surface as a functional of the total intrusion $(\Delta z+\delta)$ and the number of carbons in the domain N_d. The red line represents the minimal ascending path from the starting graphite to the present structure, just a guide for the eyes. (b) The cross-sectional view of the adiabatic energy surface at $N_d=26$. In the real process, the diaphite is realized through the Franck-Condon excitation and the lattice relaxation process therefrom. (c) The N_d dependency of the height of the barrier and the local minimum. (d) The estimated diaphite structure. The values are given in angstrom unit (Å).

will be explained in detail in Fig. 2(b). As seen in Fig. 2(a), the second minimum has appeared at $N_d=26$ and the total intrusion 0.57 Å. The local shear displacement does not give an energy gain in the present case; $\Delta x=0$.

In Fig. 2(c), we can see the height of the barrier and the local minimum for various domain sizes. Simply speaking, the minimal domain size is determined by the competition between the decrease in the incommensurate energy and the increase in the deformation energy. As a result, the height of the barrier takes a minimum value at $N_d=26$.

The cross-sectional view of Fig. 2(a) at $N_d=26$ is given in Fig. 2(b). The height of the barrier is 3.43 eV with the total intrusion 0.50 Å. The diaphite structure is obtained at the energy 3.30 eV with the total intrusion 0.57 Å ($\Delta z=0.50$, $\delta=0.07$). Thus, the diaphite structure has appeared at the energy 0.13 eV lower than that of the top of the barrier, and it is sufficient to stabilize this structure against the thermal fluctuation at around room temperature. The estimated diaphite structure at the domain center is given in Fig. 2(d). The averaged interlayer distance has contracted up to 2.35 Å from the original 3.35 Å.

To confirm the formation of the interlayer covalent bond at the diaphite structure, we have examined the Mulliken's overlap population analysis[22] for carbons that form the interlayer bond. The overlap population at the graphite is almost zero. While, this value increases together with the contraction of the interlayer distance and becomes 0.002 at the top of the barrier. At the diaphite structure, the value becomes 0.031. It is still small but takes about 15 times larger value than the value at the top of the barrier, due to the effect of the buckling. The bond order at the diaphite structure becomes 0.1. Then the carbons which belong to different layers are weakly but clearly bounded, although the sp^2 nature is still dominant.

Roughly speaking, the height of the barrier is twice of the energy of the irradiated light. Then it needs three or more light quanta to overtake this barrier. Thus, we can conclude that the energy barrier between the starting graphite and the minimal diaphite can be overtaken by few visible photons. The system excited by few visible photons is expected to reach this local minimum (nearest second minimum) of the diaphite through the lattice relaxation process, as schematically depicted in Fig. 2(b).

It should be noted that this estimated minimal diaphite domain will proliferate stepwise to larger domains, transferring various local minima of the adiabatic potential with further structural changes, by further additional visible photon excitations, and finally reach the nanosize domain that was observed in the experiment. Once the state reaches a local minimum of the adiabatic potential, this state has a long lifetime, since each local minimum of the adiabatic potential is sufficiently stable against the thermal fluctuation at around room temperature. This stepwise or iterative proliferation of domains is quite in contrast to the instantaneous nucleation of a large domain that needs tremendous energy, as already described in connection with the conventional uniform phase transition.

In some cases, the STO-3G basis may not fit for the calculation of the structure optimization. However, the expected error coming from the cluster size is larger than that coming

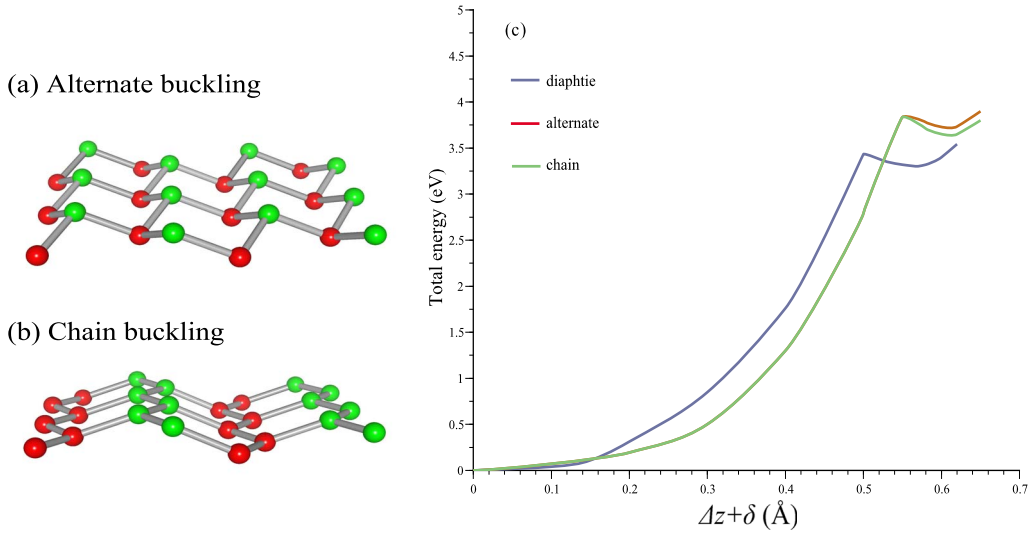

FIG. 3. (Color online) (a) An alternate buckling; carbons alternately sink down and rise up in each six-membered ring. (b) Chain buckling; half of carbons sink down and others rise up, forming the *cis*-type zigzag chain, in each six-membered ring. (c) The adiabatic energy for each buckling path. The given paths are at N_d=24 for the alternate and the chain bucklings. The path for the diaphite buckling is the same with that in Fig. 2(b).

from the basis size in the present problem, and our main conclusion will not be affected even if the highly accurate basis, i.e., 6–31G,[23] is used.

III. ADIABATIC PATHS WITH COMPETITIVE DISTORTION PATTERNS

Let us now examine the relative stability of the diaphite structure by comparing it with other possible distortion patterns. We have considered two different buckling structures, which are given in Fig. 3. One is the alternate buckling; carbons in each six-membered ring rise up and sink down alternately. Another is the chain buckling; the half of carbons in each six-membered ring rise up and others sink down, forming the *cis*-type zigzag chain. The way of the total-energy calculation is the same with the diaphite case except the bucklings.

Results are given in Fig. 3(c). The lowest barrier is given at N_d=24 for the alternate and the chain bucklings. In both cases, the height of the barrier is 3.83 eV with the total intrusion 0.55 Å. The local minima have appeared at the energy 3.73 and 3.65 eV for the alternate and chain bukclings, respectively, with the total intrusion 0.62 Å (Δz =0.55, δ=0.07). By comparing these results with the diaphite case, we can conclude that the path with the diaphite buckling gives the lowest barrier and also the most stable state. One of its reasons is the smaller degrees of deformation. The diaphite buckling is realized by one third of carbons that sunk down in each six-membered ring. On the other hand, half of carbons must sink down to realize the other buckling states.

IV. ELECTRONIC STATE OF THE DIAPHITE

The electronic state of the diaphite has been estimated by means of the TB approximation with the SK parametrization.[15] The carbon system has six SK parameters: ϵ_s, ϵ_p, $V_{ss\sigma}$, $V_{sp\sigma}$, $V_{pp\sigma}$, and $V_{pp\pi}$, which are the binding energies of 2*s* and 2*p* orbitals and the hopping integrals for 2*s*-2*s* σ coupling and so on. We use the 2*s* and 2*p* orbital energies obtained from the LDA calculation for ϵ_s and ϵ_p because these values are not so sensitive against structural changes. The hopping integrals are fitted so as to reproduce the width of the σ and π bands and the energy gap by the LDA for the graphite and the diamond. The optimized SK parameters are given in Table I. For the bond-length ($\equiv r$) dependency of hopping integrals, we have applied the Harrison's r^{-2} scaling rule,[24]

$$V(r) = V(r_0)\left(\frac{r_0}{r}\right)^2, \tag{1}$$

where r_0 is the reference bond length and we have fixed it to 1.54 Å. The calculation has been performed on the cluster which consists of two layers and each layer contains 2592 carbons. Interactions are taken into account up to the nearest neighbors and the periodic boundary condition is applied.

Here we mention that it is possible to estimate the electronic states by using the Kohn-Sham (KS) orbitals obtained from the LDA calculation. However, in the present calculation, the number of the KS orbitals is not enough to obtain the clear density of states (DOS), but only spiky lines are obtained. Moreover it is important to treat the itinerant prop-

TABLE I. The estimated SK parameters (eV) at r_0=1.54 Å.

$\epsilon_p-\epsilon_s$	8.346
$V_{ss\sigma}(r_0)$	−4.143
$V_{sp\sigma}(r_0)$	5.689
$V_{pp\sigma}(r_0)$	7.758
$V_{pp\pi}(r_0)$	−2.489

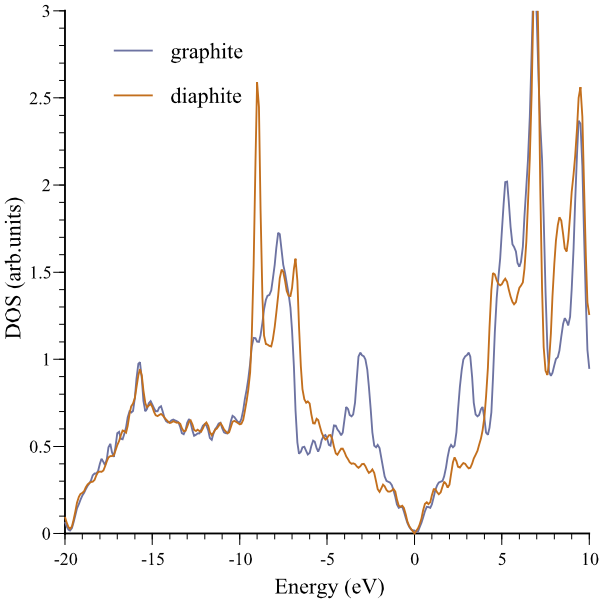

FIG. 4. (Color online) The DOS for the graphite and the diaphite. The zero of energy is the Fermi energy of each state.

erty of π orbitals correctly because the diaphite domain is really surrounded by the semimetallic continuum of the graphite phase. Then we use the TB approximation for the evaluation of the DOS that gives consistent results with the LDA.

The DOS, thus evaluated, is given in Fig. 4. The zero of energy is the Fermi energy of each state. The graphite exhibits its specific semimetallic V-shaped structure around the Fermi energy. The π and π^* orbitals compose the top of valence band and the bottom of conduction band, respectively, and have peaks at ± 3.1 eV. At the diaphite, the behavior of the DOS within ± 1.5 eV is almost the same with the graphite; but peaks at ± 3.1 eV are lost and the DOS near the Fermi energy is totally reduced. Then the electronic state of the diaphite has a pseudogap, characteristic to the insulator immersed in the semimetal. According to the increase in the domain size by additional photoirradiation, the sp^3 nature will dominate and the band gap at the Fermi energy will be opened.

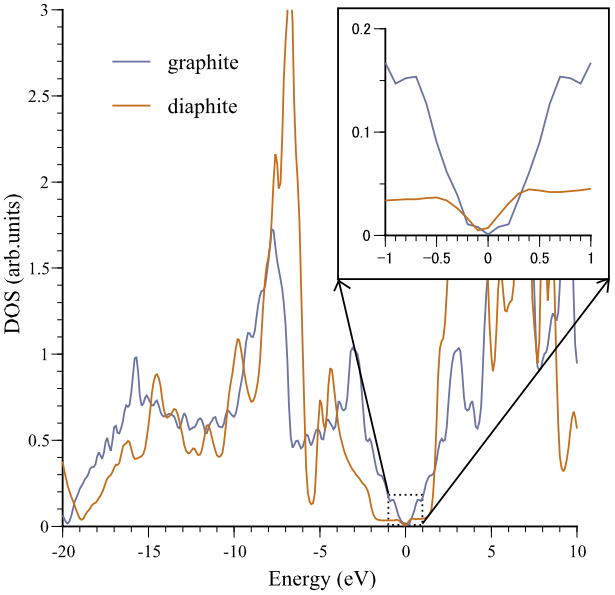

FIG. 6. (Color online) The DOS at the diaphite structure (at the second local minimum) in Fig. 5(a). In the small inset, the DOS at the energy range from −1 to 1 eV is zoomed. The zero of energy is the Fermi energy of each state.

V. HIGHER-ENERGY STATE WITH A SHEAR DISPLACEMENT

In Secs. I–IV, we have clarified the nucleation of the minimal diaphite domain in the graphite. After overtaking the initial barrier, further additional structural changes are expected to occur by further photoexcitations, and their nature will be different from the aforementioned minimal domain. The diaphite includes more than 1000 carbons and has appeared after the 10^4 shots of the laser irradiation in the experiment.[5] Its nature will be also different from the minimal diaphite. Especially, the local shear displacement is detected in the STM measurement.

Here, let us clarify the state with finite shear displacement ($\Delta x \neq 0$). For its purpose, we have performed the total-energy calculation with a large domain (N_d=256) by using the same cluster.

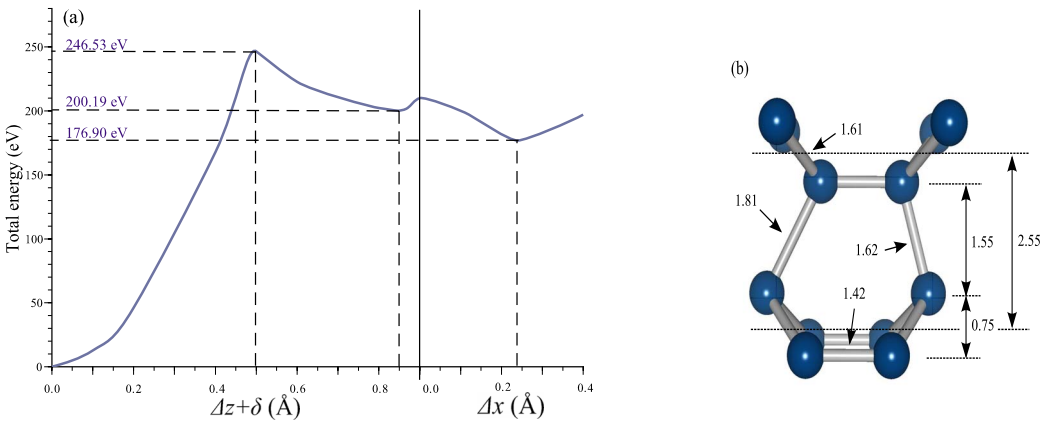

FIG. 5. (Color online) (a) The adiabatic path to a large diaphite domain. The horizontal axis is separated to two parts. At the first part, the energy is plotted as a functional of the total intrusion. In the second part, the energy is plotted as a functional of the local shear displacement with the total intrusion 0.9 Å. (b) The estimated diaphite structure. The values are given in angstrom unit (Å).

The estimated adiabatic path with the above assumption is given in Fig. 5(a). The local shear displacement is introduced and the total energy is plotted with its value at the domain center in the second part of horizontal axis. After overtaking the initial barrier with the energy 246.63 eV, the first local minimum has appeared at the energy 200.19 eV with the total intrusion 0.85 Å (Δz=0.35, δ=0.50) and Δx=0.00. The second local minimum has appeared at the energy 176.90 eV with the finite shear displacement. The estimated parameters for the deformation are Δz=0.40 Å, δ=0.50 Å, and Δx=0.24 Å. Its structure is given in Fig. 5(b). Then the averaged interlayer distance has contracted up to 2.55 Å, and the structure is stabilized due to the effects of the large buckling and the local shear displacement.

The DOS at the second local minimum is given in Fig. 6. The system has opened the band gap at about 3 eV although some fractional states remain inside of the gap. This DOS inside of the gap is zoomed as the small inset of Fig. 6. The small peaks have appeared at around $\pm$0.5 eV and those behaviors are in good agreement with the experiment.[5] Then the diaphite states have become an insulator.

VI. CONCLUSION

We have, thus, estimated the adiabatic path to photoinduce the diaphite from the graphite by means of the *ab initio* total-energy calculation. The height of the minimal barrier becomes 3.43 eV, and it is able to be overtaken by few visible photons. The minimal diaphite structure appears after overtaking this initial barrier and is sufficiently stable against the thermal fluctuation at around room temperature. The electronic state of the diaphite is also clarified by means of the TB approximation with the SK parametrization, and we have shown a pseudogap to open. We also examined large domain states, in which the sp^3 nature dominates through the large buckling and the finite local shear displacement. In this case, the diaphite becomes an insulator.

ACKNOWLEDGMENTS

The authors thank K. Tanimura and J. Kanasaki for presenting their research results prior to publication and valuable discussions. The authors also thank S. Tsuneyuki and K. Terakura for helpful discussions. This work is supported by the Ministry of Education, Culture, Sports, Science and Technology of Japan, the peta-computing project, and Grant-in-Aid for Scientific Research (S) under Grant No. 19001002, 2007.

*ohni@post.kek.jp

[1] K. Nasu, *Photoinduced Phase Transitions* (World Scientific, Singapore, 2004).
[2] K. Nasu, Rep. Prog. Phys. **67**, 1607 (2004).
[3] K. Yonemitsu and K. Nasu, Phys. Rep. **465**, 1 (2008).
[4] L. Radosinski, K. Nasu, J. Kanazaki, K. Tanimura, A. Radosz, and T. Luty, *Molecular Electronic and Related Materials-Control and Probe with Light*, edited by T. Naito (Trans-world Research Network, India, 2008).
[5] J. Kanasaki, E. Inami, K. Tanimura, H. Ohnishi, and K. Nasu Phys. Rev. Lett. (to be published).
[6] R. K. Raman, Y. Murooka, C. Y. Ruan, T. Yang, S. Berber, and D. Tomanek, Phys. Rev. Lett. **101**, 077401 (2008).
[7] D. W. Brenner, Phys. Rev. B **42**, 9458 (1990).
[8] S. Fahy, S. G. Louie, and M. L. Cohen, Phys. Rev. B **34**, 1191 (1986).
[9] S. Fahy, S. G. Louie, and L. M. Cohen, Phys. Rev. B **35**, 7623 (1987).
[10] Y. Tateyama, T. Ogitsu, K. Kusakabe, and S. Tsuneyuki, Phys. Rev. B **54**, 14994 (1996).
[11] F. Bundy, J. Chem. Phys. **38**, 631 (1963).
[12] T. Irifune, A. Kurio, S. Sakamoto, T. Inoue, and H. Sumiya, Nature (London) **421**, 599 (2003).
[13] F. Banhart, J. Appl. Phys. **81**, 3440 (1997).
[14] H. Nakayama and H. Katayama-Yoshida, J. Phys.: Condens. Matter **15**, R1077 (2003).
[15] J. C. Slater and G. F. Koster, Phys. Rev. **94**, 1498 (1954).
[16] J. C. Slater, Phys. Rev. **81**, 385 (1951).
[17] S. H. Vosko, L. Wilk, and M. Nusair, Can. J. Phys. **58**, 1200 (1980).
[18] W. J. Hehre, R. F. Stewart, and J. A. Pople, J. Chem. Phys. **51**, 2657 (1969).
[19] M. W. Schmidt, K. K. Baldridge, J. A. Boatz, S. T. Elbert, M. S. Gordon, J. J. Jensen, S. Koseki, N. Matsunaga, K. A. Nguyen, S. Su, T. L. Windus, M. Dupuis, and J. A. Montgomery, J. Comput. Chem. **14**, 1347 (1993).
[20] P. M. W. Gill, B. G. Johnson, and J. A. Pople, Chem. Phys. Lett. **209**, 506 (1993).
[21] P. Pulay, J. Comput. Chem. **3**, 556 (1982).
[22] R. S. Mulliken, J. Chem. Phys. **23**, 1833 (1955).
[23] R. Ditchfield, W. J. Hehre, and J. A. Pople, J. Chem. Phys. **54**, 724 (1971).
[24] W. A. Harrison, *Electronic Structure and the Properties of Solids (The Physics of The Chemical Bond)* (Dover, New York, 1980).